Journal of Energy Storage 83 (2024) 110618

Contents lists available at ScienceDirect

Journal of Energy Storage

journal homepage: www.elsevier.com/locate/est

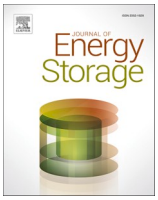

Research papers

Thermal energy storage for direct steam generation concentrating solar power plants: Concept and materials selection

Cristina Prieto [a,*], Luisa F. Cabeza [b], M. Carmen Pavón-Moreno [a], Elena Palomo [c,d]

[a] Department of Energy Engineering, Universidad de Sevilla, 41092 Sevilla, Spain
[b] GREiA Research Group, Universitat de Lleida, Pere de Cabrera s/n, 25001 Lleida, Spain
[c] Center for Cooperative Research on Alternative Energies (CIC energiGUNE), Basque Research and Technology Alliance (BRTA), Alava Technology Park, Albert Einstein 48, 01510 Vitoria-Gasteiz, Spain
[d] IKERBASQUE, Basque Foundation for Science, Plaza Euskadi 5, 48009 Bilbao, Spain

ARTICLE INFO

Keywords:
Direct steam generation (DSG)
Concentrating solar power (CSP)
Thermal energy storage (TES)
Long-term
Phase change material (PCM)

ABSTRACT

Direct steam generation (DSG) concentrating solar power (CSP) plants uses water as heat transfer fluid, and it is a technology available today. It has many advantages, but its deployment is limited due to the lack of an adequate long-term thermal energy storage (TES) system. This paper presents a new TES concept for DSG CSP plants. This system is based on three blocks, a saturated block based on phase change materials, an overheating block that elevates the vapor temperature of a heat transfer fluid to the desired values, and a preheating block that increases the temperature difference between a cold tank and a hot tank of a non-phase change thermal storage material. After a deep selection and characterization process, the material to be used is LiOH/KOH, since although it has the disadvantage of high corrosion, the identified advantages overcome it as an ideal PCM for this process.

1. Introduction

Concentrating solar power is a technology that uses mirrors to reflect and concentrate solar energy onto a receiver, heating a fluid up to high temperature. This heat can be used to spin a turbine or to power an engine to generate electricity [1]. These plants can be configured as power tower systems, which arrange mirrors around a central tower that acts as receiver, or in linear systems where rows of mirrors concentrate the solar energy onto parallel tube receivers, as well as solar dishes that use a parabolic dish of mirror.

In direct steam generation (DSG) concentrating solar power (CSP) plants, water is used as heat transfer fluid (HTF). This technology is commercially available today and it has the advantage in front of those using molten salts as HTF of eliminating the need of intermediated HTF, therefore, plants have a higher overall plant efficiency and are more environmentally friendly [2,3]. In these plants, the steam is produced in the receiver thanks to the solar energy reflected from the heliostat field and it is fed directly to the power block, which also means lower investment costs. Another advantage of this technology is that the limitation of other HTF temperatures disappear (i.e., limit of 400 °C in parabolic through plants using thermal oil, or limit of 565 °C in tower plants using molten salts as HTF), therefore higher temperatures can be reached, which would allow the use of more efficient power cycles [4]. However, this technology presents a series of drawbacks, such as the need for more robust pipes and elements to withstand high pressures, especially for Fresnel or parabolic troughs, more complex control systems, due to the two-phase flow existing in receiving tubes. A key constraint of this technology is the absence of a high-capacity competitive storage system [2].

The standard power cycles for these superheated steam plants typically adhere to Rankine cycles, with or without reheat, operating within a pressure range of 100 bar to 170 bar. The superheating temperatures span from 585 °C to 360 °C. These cycles are optimized for daily operation, incorporating extraction and recuperation setups to enhance performance during daylight hours when electricity generation takes place. Simultaneously, these configurations allow for the storage system to be charged if conditions permit.

The known storage systems associated with these plants are thermal storage systems accommodating heat from both saturated and superheated steam. The performance during discharge is somewhat compromised due to discharging steam at pressures and/or temperatures significantly below nominal values. These systems are designed to work with superheated steam cycles, suitable for turbines that exclusively accept superheated steam. In this scenario, discharged steam must

* Corresponding author.
E-mail address: cprieto@us.es (C. Prieto).

https://doi.org/10.1016/j.est.2024.110618
Received 30 August 2023; Received in revised form 15 January 2024; Accepted 18 January 2024
Available online 1 February 2024
2352-152X/© 2024 The Authors. Published by Elsevier Ltd. This is an open access article under the CC BY license (http://creativecommons.org/licenses/by/4.0/).

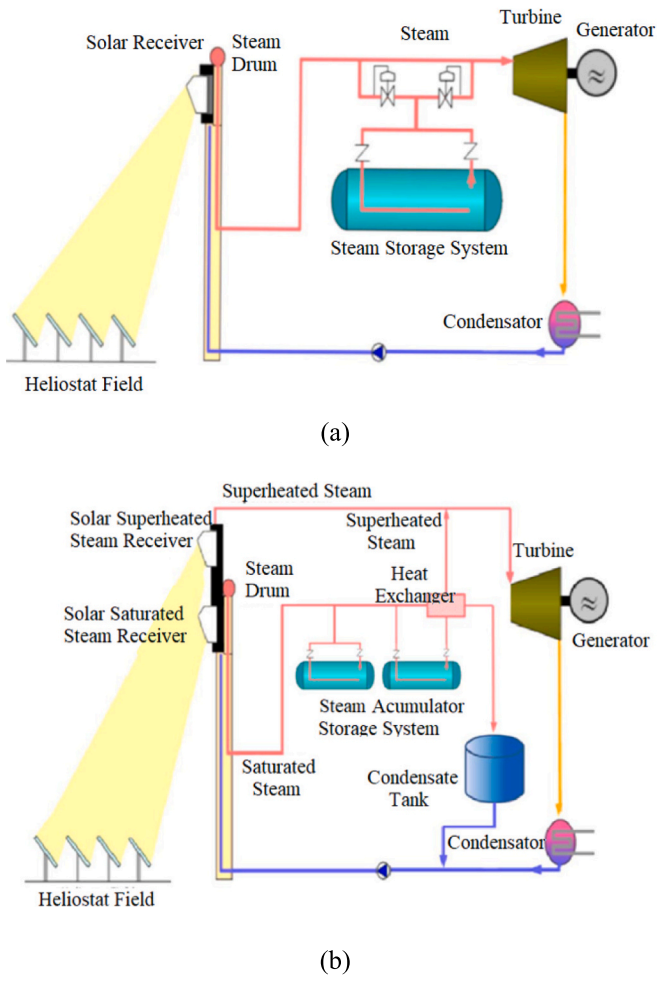

Fig. 1. Flow diagram of a direct steam generation (DSG) tower plant with steam accumulator as TES system [2].

Table 1
Specifications of the CSP plant to integrate the TES system.

Nominal electrical power	≥50 MW
Receiver technology	Direct Steam Generation Parabolic Trough
Heat transfer fluid (HTF)	Water/steam
Thermal energy storage (TES) technology	Latent TES with phase change materials (PCM)
Thermal energy storage capacity	≥300 MWh, ≥6 h
Steam cycle	Superheated steam at 450 °C and 95,115 bar

uphold a minimal superheating temperature for each operational pressure. Generally, this requires the discharged steam to be approximately 50 °C above the saturation temperature.

Presently, superheated steam plants are predominantly designed with thermal storage systems based on saturated steam accumulators, often referred to as "Ruth's tanks" [5]. These tanks have the capacity to store steam at the same pressure during charging but allow for discharge only at significantly lower pressures than nominal values. Discharge can occur through either a sliding pressure mechanism or via constant pressure steps within the saturation module [6,7].

An alternative thermal storage configuration involves two molten salt tanks—designated as the cold and hot tanks—without vapor accumulation. A heat exchanger connects these tanks, with the discharge process involving the evaporation and superheating of water from the power cycle. This is achieved through the transfer of salts from the hot tank to the cold tank, facilitated by the heat exchanger. During charging, superheated steam is introduced into the heat exchanger. As this steam cools and partially condenses, it exchanges heat with the salts moving from the cold tank to the hot tank via the heat exchanger. This setup also integrates a heat recuperator that utilizes the heat of the outgoing salt stream from the heat exchanger during charging. The recuperator is crucial for fully condensing the partially condensed steam in the heat exchanger. However, this configuration with the recuperator mandates modifications to the power cycle's extraction conditions, causing deviations from nominal operation and subsequently affecting maximum attainable efficiency [3]. These are active direct storage systems where the steam is stored at high temperatures in the tanks.

In 2023, only four commercial plants using steam as HTF with tower technology and with direct steam accumulators are working. The first two plants were PS10 and PS20, built by Abengoa in Spain in 2007 and 2009, respectively. Then Khi solar One and Ivanpah Solar were built with the same technology [8].

PS10 and PS20 are located in Sanlúcar la Mayor, Sevilla (Spain); they have a nominal capacity of 11 MW and 20 MW, respectively, and an expectation generation of 23.4 and 48 GWh/year, respectively. Khi solar One started its operation in 2012, and it is located in Northern Cape (South Africa); it has a nominal capacity of 50 MW and an expectation generation of 180 GWh/year. Ivanpah Solar started its operation in 2014, and it is located in Primm, California (United States of America); it has a nominal capacity of 377 MW and an expected generation of 1079 GWh/year [9].

The schematic flow diagram of a direct steam generation tower plant with steam accumulator is shown in Fig. 1a. In this system, the excess steam produced by the receiver is stored in direct steam accumulators. This technology is used in PS10, where the equivalent to an effective operational capacity of 50 min at 50 % turbine workload is installed (20 MWh of storage capacity) [10]. In this plant, the system has 4 storage tanks used sequentially and the stored energy is used to cover transient periods.

Khi solar One uses superheated steam to reach higher temperatures and feed the turbine at 540 °C and 130 bars, increasing the power cycle electrical efficiency 30 % compared to PS20. The storage capacity of the plant is 2 h, and it comprises 19 steam accumulator tanks (Fig. 1b).

Therefore, the main challenge of DSG CSP plants is to develop a storage system that allows longer storage capacity for longer periods of time, similar to those used in CSP plants using molten salts or thermal oil as HTF [11]. With such storage concept, the advantages of the two CSP technologies would remain, bringing a new generation of more efficient and more environmentally friendly CSP plants, maintaining a higher level of dispatchable due to the presence of these large capacity storage systems. The aim of this paper is the development of this TES concept for DSG CSP plants that mitigates the effect of loading and/or unloading under conditions differing from nominal by introducing a system composed of three blocks: (i) a saturated block based on phase change materials, (ii) an overheating block that elevates the vapor temperature of a heat transfer fluid to the desired values, and (iii) a preheating block that increases the temperature difference between a cold tank and a hot tank of a non-phase change thermal storage material. The non-phase change thermal storage material is the well-known molten salts, and this work develops the best solutions for the saturated block.

2. Thermal energy storage concept for a direct steam plant with parabolic trough technology

The specifications of the CSP plant are presented in Table 1 and the working conditions in Fig. 2. When the TES tank is discharged, the water enters at about 170 °C following the entropy-temperature diagram presented in Fig. 3. The water is first heated up to the vaporization corresponding to the working temperature (~308 °C), this temperature has to be below the PCM melting temperature. Then it is evaporated at constant temperature, and finally the resulting steam is overheated to reach the working temperature of the turbine (~450 °C). Preliminary

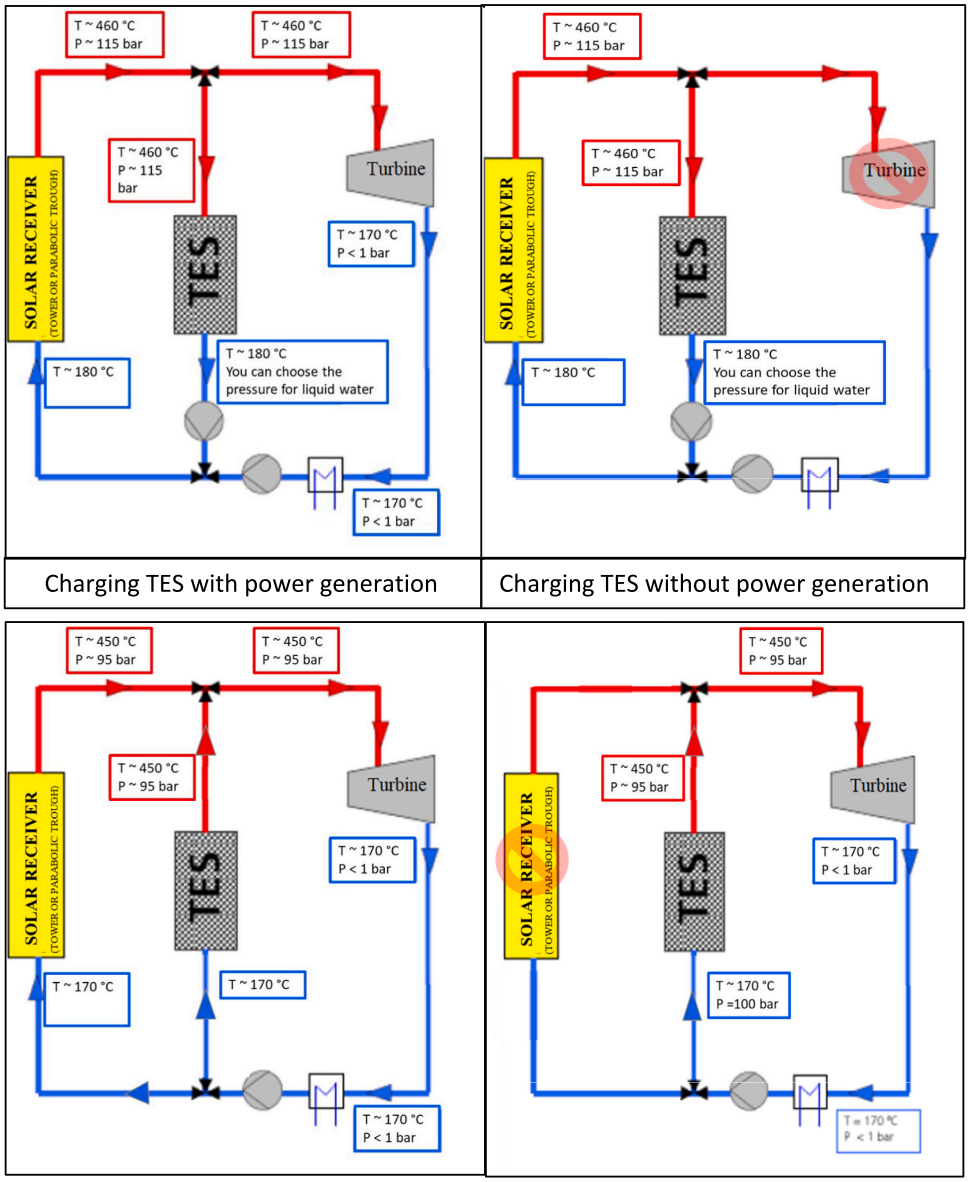

Fig. 2. Operating conditions of the proposed TES system.

estimations say that during the discharge process, 35 % of the energy is used for water preheating, 60 % for water evaporation, and 15 % for steam superheating. During the charging process, the overheated steam produced by the solar field (~460 °C) is cooled down to around 322 °C, when it condensates at constant temperature that has to be above the PCM melting temperature, and finally the resulting water is cooled down until the inlet temperature of the solar field is reached (~180 °C).

In the charge mode of the PCM block with saturated steam, the pressure will typically increase as the steam is introduced and the PCM undergoes a phase change (from a solid to a liquid). The pressure required for charging is influenced by factors such as the temperature at which the phase change occurs and the specific properties of the PCM.

During discharge, when the PCM releases the stored energy (usually in the form of latent heat) and transitions back to its original phase, the pressure may decrease. The discharge pressure will depend on various factors, including the rate of energy extraction and the specific conditions of the discharge process. To ensure reasonable power performance, a minimum temperature difference in temperature and pressure must be guaranteed between the evaporation/condensation temperatures, depending on the case, and the PCM melting temperature, as shown in the diagram in Fig. 3.

A typical T–s diagram for charging and discharging of steam in a power plant is provided in Fig. 3 [12]. As can be seen in the figure, the thermal match between the storage system and working fluid are maximized when steam production, which is an isothermal process, is coupled with an isothermal storage process. Being that latent heat storage is isothermal, it is deemed advantageous to use this type of system for the evaporation of steam.

In the development of TES systems, the HTF used, and its working conditions have a big impact. In the DSG solar power plants, the TES charge and discharge need to consider the preheating and superheating steps, when the HTF is single phase with the temperature difference according to the energy transferred.

Therefore, the TES concept presented here demands the combination of several segments or modules, as shown in Figs. 4 and 5. The saturated block is based on the latent heat of a material that undergoes a phase change at a temperature that should be kept as close as possible to the steam condensing/evaporating temperature, ensuring at the same time a minimum temperature difference to achieve reasonable power performances.

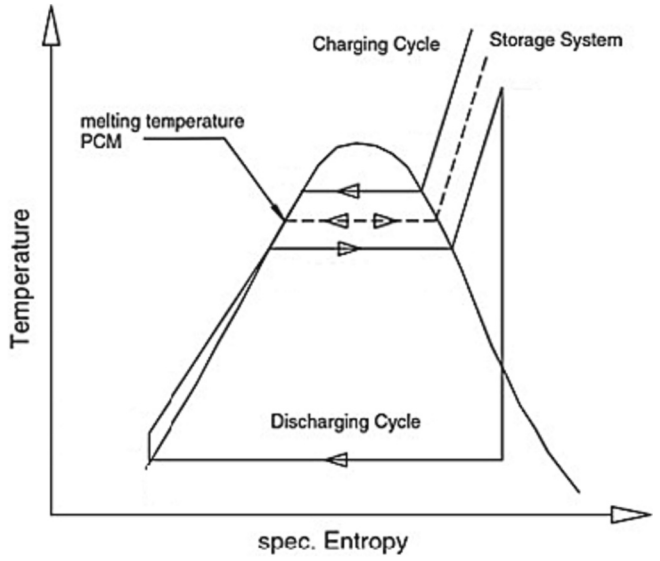

Fig. 3. Entropy-temperature diagram of water following the TES system studied [12].

The preheating block facilitates, during discharge, the thermal exchange between the non-phase change thermal storage material from an overheater and the heat transfer fluid from the power cycle. In this way, the non-phase change thermal storage material reduces its temperature to the minimum allowed without undergoing a phase change. This increase in temperature difference within the non-phase change thermal storage material between the cold and hot tanks, up to maximum values, enables the utilization of a smaller quantity of the material. This fully exploits the available temperature range and thereby reduces investment costs, both for the material itself and for tank volume and foundations.

The overheating block is responsible for raising the temperature of vapor originating from the saturated block to values as close to nominal as possible. The superheated steam module oversees steam overheating from ~310 °C to ~450 °C. Salts undergoing melting over such an interval of temperature (~310–450 °C), as well as salts with different melting points so that they allow forming a suitable cascade of PCM within ~[310–450 °C], will be investigated as storage medium. As efficiency of energy transfer between the HTF and the PCM (convection) is highly reduced compared to evaporation/condensation, a suitable heat exchanger configuration must be searched too.

The proposed configuration includes a phase change module, a cold tank for non-phase change thermal storage material (cold tank), a hot tank for non-phase change thermal storage material (hot tank), an overheater that performs heat exchange between the non-phase change thermal storage material and the superheated vapor state heat transfer fluid, and a preheater that performs exchange between the non-phase change thermal storage material and the subcooled liquid state heat transfer fluid.

During discharge, following the heat transfer fluid circuit, both heat exchangers are installed in series with the phase change module, and in the direction of decreasing temperature, they are arranged as follows: preheater, phase change module, and overheater. The phase change module is used to evaporate the liquid or condense the vapor, depending on whether the system is in discharge or charge mode, respectively.

A Piping and Instrumentation Diagram (P&ID) is shown in Fig. 5, which represents the concept of modular storage that has been previously explained in both the charging and discharging modes, as well as

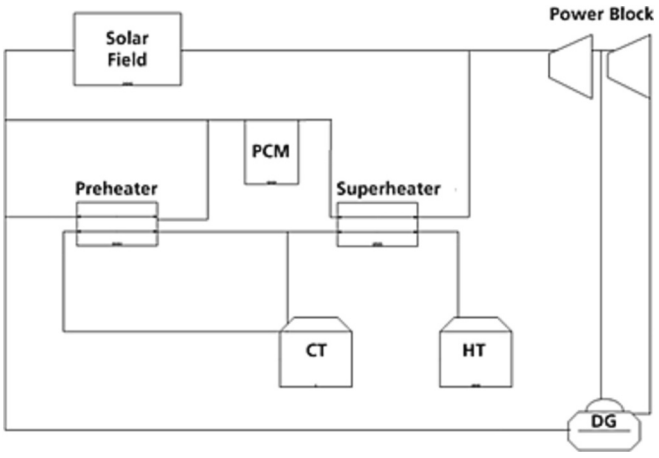

Fig. 5. DSG CSP plant with the new TES concept.

Table 2
Selection criteria for the storage media.

Criteria		Requirement
Physical	Phase change temperature	Fitting the process requirements
	Latent heat	As high as possible
	Volume expansion during melting	As low as possible
	Sub-cooling	Negligible
	Segregation risk	As low as possible
	Thermochemical stability	To warrant long enough life
Technological	Danger, toxicity	As low as possible
	Corrosion power, hygroscopicity	As low as possible
	Cost	As low as possible
	End of life	Recyclable if possible

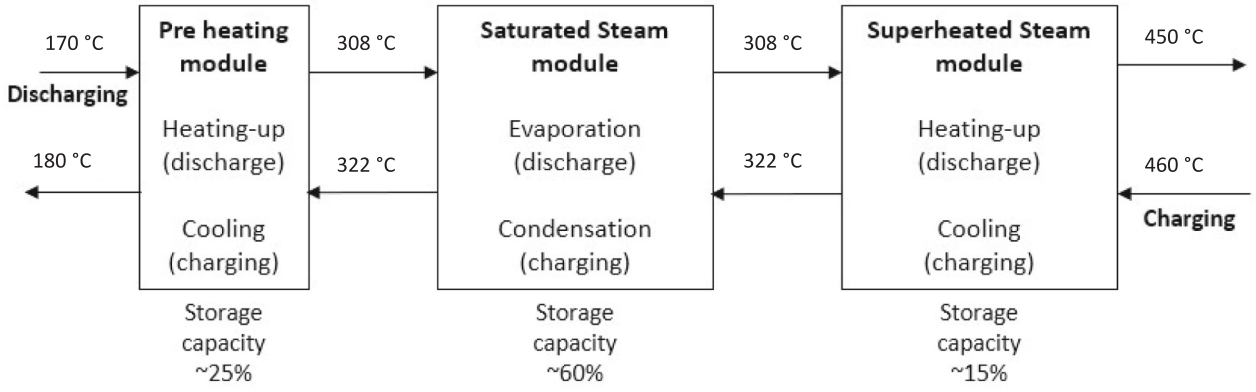

Fig. 4. Concept of the TES system developed.

Table 3
Databases used to get information for storage media.

Database	Information obtained
Data base from the ECES (Energy Conservation trough Energy Storage) program of the IEA (International Energy Agency) http://www.fskab.com/Annex17/ (Excel file)	Formula and composition of the salt, melting point, latent heat and relative volume expansion.
"Tohoku molten salt data base – Eutectic finder" (Software) Developed by the University of Tokyo in collaboration with the Yamamura laboratory http://ras.material.tohoku.ac.jp/~molten/molten_eut_query1.php	Allows automatic searching of salts melting at a given temperature or salts melting within a chosen range of temperatures.
"Chemexper Chemical Directory" (Web Site) Catalogue on-line from >30 suppliers of chemical products http://www.chemexper.com/	Name, chemical formula, molecular mass, CAS number, security card, melting temperature, boiling point, density, etc.
"ACerS – NIST Phase Equilibria Diagrams" Data base distributed by the American Ceramic Society http://www.ceramics.org/	A very large data base of phase equilibria diagrams and bibliography.
NIST Laboratory data base	Density, conductivity, viscosity and surface tension for pure salts, binary systems and ternary systems.
Information sent by Alfa Aesar	List of their products with melting point in the interval 290–310 °C.
Information sent by GTT-Technologies	260 phase equilibria diagrams.

Table 4
Potential candidates to be used as storage media in the saturated steam module.

Formulae	Composition (wt%)	Melting point (°C)	Latent heat (kJ/kg)	Relative volume expansion (%)	Considered?
LiOH-LiBr	45.27–54.73	303.9	802.8	11.5	Yes
LiOH-KOH	46.05–53.95	314	534.8	6.9	Yes
LiOH-LiCl	36.1–63.9	314	338.0	19.7	Yes
NaSCN	100	307	297.8	n.a.	No
NaOH-Na_2SO_4	81.5–18.5	294.4	287.0	19.0	Yes
$FeCl_3$	100	300	266.0	0.02	No
$FeCl_2$-$FeCl_3$	10.63–89.37	293.4	251.1	43.9	No
NaCl-$NaNO_3$	4.70–95.30	297.5	189.1	19.8	No
NaBr-$NaNO_3$	10.90–89.1	291	186.0	20.0	No
NaF-$NaNO_3$	1.27–98.73	304	184.0	19.0	No
Na_2CO_3-$NaNO_3$	2.27–97.73	306.5	181.5	19.0	No
$NaNO_3$-Na_2SO_4	91.89–8.11	298.8	179.0	19.5	No
$NaNO_3$	100	309	178.5	18	–

its connections with the solar field and the power block.

3. Materials and method

3.1. Materials selection

For the latent heat module, the main criteria used to select the storage media (PCM) are presented in Table 2. The first screening was mainly carried out using phase change temperature, latent heat, and volume expansion criteria. Danger and toxicity have been used not to rank but to exclude highly dangerous products. As getting realistic information for salts prices is a tricky task, cost was not considered is this first analysis.

For the saturated steam module, salts undergoing melting at constant temperature have to be used: pure salts or mixtures at special concentrations (e.g., eutectics points). For the superheated steam module, two main concepts will be investigated:

- A set of salts in cascade. This means looking for as many salts undergoing melting at constant temperature as necessary for a suitable covering of the interval defined by the temperature of water vaporization (~310 °C) and the inlet temperature to the turbine (~450 °C).
- A single PCM undergoing phase change over the interval of temperature above mentioned. Phase diagrams showing suitable points for spread melting or thermo-adjustability properties (see figures below) will be investigated.

To identify appropriate salts for saturated steam and superheated steam storage modules some handbooks and research reports [13–15], some free databases (Table 3) and FactSage 7.3® software was used. FactSage is the result of over 25 years of collaborative efforts between Thermfact/CRCT (University of Montreal, Canada; www.crct.polymtl.ca) and GTT-Technologies (Aachen, Germany; www.gtt-technologies.de). It integrates a very large data base of salts with main thermodynamic functions and properties, as well as thermo-chemical models allowing estimation of phase equilibria diagrams for multicomponent systems. In the framework of this study, FactSage was intensively used to:

- Calculate phase equilibria diagrams for binary or ternary systems. We remind that a phase diagram is a synthetic view (e.g., in a temperature/composition plane for isobaric transformations) of the system equilibria. Lines represent transformations (e.g., solid-liquid) and regions between lines are defined by the corresponding mixture of phases and their respective chemical compositions. A phase diagram allows e.g., quick identification of transition temperatures, particular points of interest (e.g., eutectics) and so on.
- Calculate enthalpy functions and density functions at chosen points (composition) on the phase diagram and thus enthalpy change during transformations (e.g., latent heat) and relative volume expansion.

3.2. Methods

The selected materials as storage media were analysed with a differential scanning calorimeter (DSC), TG-DSC 111 SETARAM. The tests were done with a heating and cooling rate of 1 °C/min.

4. Results

4.1. Storage materials selection for the saturated steam module

As said before, search of salts for the saturated steam storage module is focused on either pure salts or binary/ternary systems with eutectic points or points where melting takes place at constant temperature. According to the fluid working pressure (~100 bar), salts showing solid-liquid transitions at 290–315 °C are being investigated.

Sodium nitrate ($NaNO_3$) was taken as a reference because long-term stability, low cost (~0.3 €/kg) and availability [16]. Melting point and latent heat are respectively 309 °C and 178 kJ/kg. Relative volume expansion during melting is however significant, about 18 % [17].

Considering required melting point (290–315 °C), 190 salts were identified using the sources described before: 40 pure salts, 100 binary systems, and 50 ternary systems. Only those with better energy performances than those of the $NaNO_3$ were kept for further analyses. They are

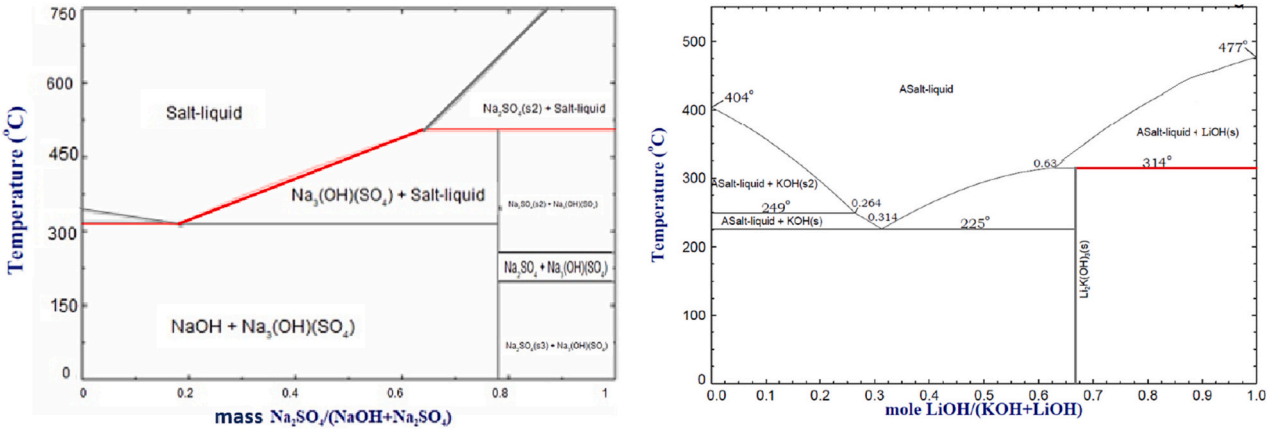

Fig. 6. Phase equilibria diagrams obtained with Fact Sage for NaOH-Na_2SO_4 (left) and LiOH-KOH (right). (For interpretation of the references to colour in this figure, the reader is referred to the web version of this article.)

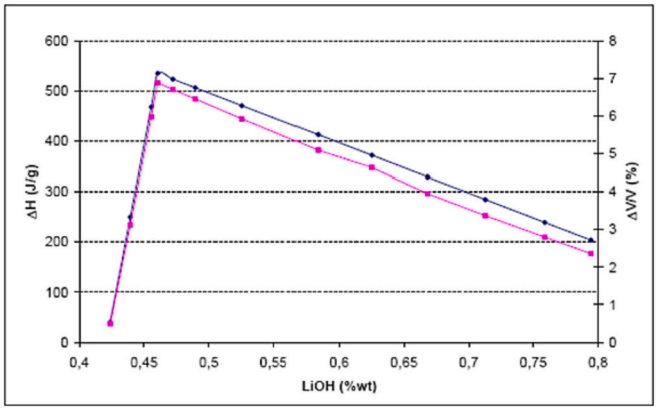

Fig. 7. Enthalpy change (blue line) and relative volume expansion (pink line) associated to a solid-liquid transformation of LiOH-KOH at 314 °C, obtained using FactSage. (For interpretation of the references to colour in this figure legend, the reader is referred to the web version of this article.)

listed and classified by decreasing latent heat in Table 4.

A second screening has been carried out considering:

- Security information. Dangerous salts like NaSCN (risk of cyanure emissions) and $FeCl_3$ (boiling temperature close to the melting point) were eliminated.
- Relative volume expansion. Salts with very high-volume expansion during melting (e.g., $FeCl_2$-$FeCl_3$) were dismissed too.
- Latent heat. Salts with non-significant latent heat improvement with regard to $NaNO_3$ have been also dismissed.

Hence, the resulting candidates for the steam saturated storage module are presented in Table 4.

From a compactness point of view, one notices that salts with LiOH are those with higher latent heat values. Indeed, relative volume expansion for LiOH-KOH is really very low.

Mixing $NaNO_3$ with $RbNO_3$ (melting point 312 °C; latent heat: 40 kJ/kg; volume expansion: none) was considered as an attempt to reduce volume expansion of $NaNO_3$. Unfortunately, the eutectic point of the resulting binary system corresponds to a very low content of $RbNO_3$ so that no significant reduction of the volume expansion was achieved.

Phase equilibria diagrams for LiOH-KOH and NaOH/Na_2SO_4 are given in Fig. 6. The selected points (eutectic or not) correspond to compositions where liquid-solid transformations take place at constant temperature.

Among LiOH-KOH compositions showing solid-liquid transformation at 314 °C (red line in the phase diagram, Fig. 6 right), the one leading to a higher enthalpy change (latent heat) was chosen. Fig. 7 shows the variations of the corresponding latent heat and the relative volume expansion regarding the binary system composition.

Fig. 8 shows the results obtained from DSC analysis. For the salt considered as reference, $NaNO_3$, peaks of crystallization (flow negative values) and melting (flow positive values) are clearly identified and they show expected forms. Measurements are repetitive enough as expected for stable behaviour; subcooling is negligible; and before melting, a small peak (at ~260 °C) corresponding to a solid-solid transformation is identified.

For the eutectic 18.5 wt% Na_2SO_4–81.4 wt% NaOH (Fig. 8b), during the two first melting/crystallization cycles, bimodal heat flux/temperature curves were observed instead of the single maximum curve characteristic of eutectics. A bimodal form usually corresponds to a melting over a temperature range, the first peak represents the eutectic melting, and it is followed by a progressive melting leading to the second pick.

For the eutectic 46.05 wt% LiOH–53.95 wt% KOH (Fig. 8c), peaks of crystallization and melting are clearly identified, and they show expected forms; measurements were repetitive; and subcooling is not very high (~2 °C).

The melting temperature (onset temperature) and latent heat (ΔH) estimated from the heat flux/temperature graphs shown in Fig. 8 are given in Table 5.

As summary:

- Results for $NaNO_3$ are in very good agreement with FactSage and literature values [18].
- Results for Na_2SO_4/NaOH disagree with FactSage values (lower melting and latent heat values).
- Results for LiOH/KOH are in good agreement with FactSage values. The small differences observed in melting point and latent heat could be explained either by the uncertainty in the sample composition or by fault DSC calibration constant (the test has been carried out without gas sweeping because a problem in the gas loop). In any case, results achieved are really interesting. LiOH/KOH is almost three times more energetic than $NaNO_3$, with low relative volume expansion (~7 % instead of 18 %) and reduced undercooling (~2 °C).

4.2. *Storage materials selection for the superheated steam module*

For the superheated steam storage module, approximate inlet and outlet HTF temperatures are 300 °C and 450 °C, respectively. Two main storage concepts will be investigated: (a) a set of salts in cascade; and (b)

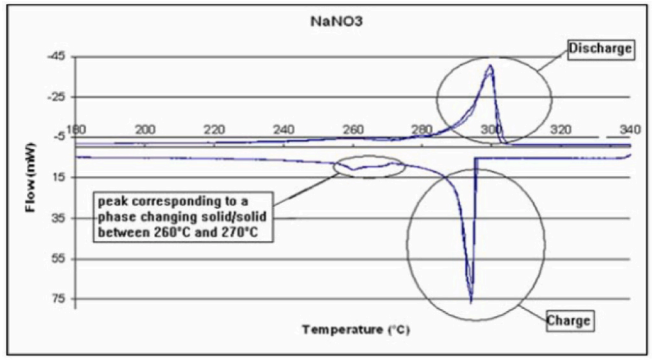

(a)

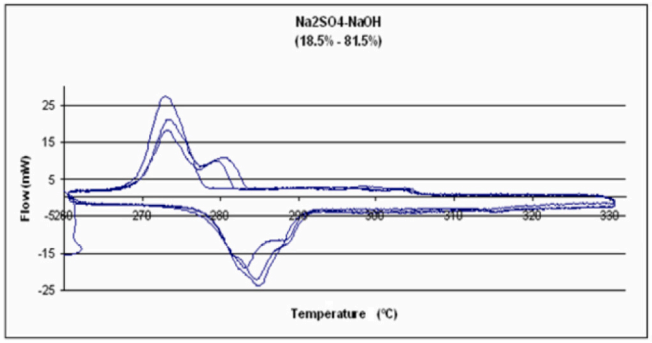

(b)

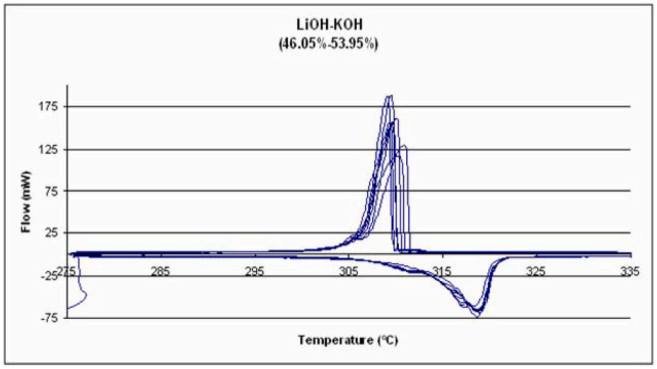

(c)

Fig. 8. DSC results for (a) $NaNO_3$, (b) Na_2SO_4 -NaOH, and (c) LiOH-KOH.

Table 5
DSC results for the selected storage media for the saturated steam module.

Salt	Melting		Solidification	
	Onset (°C)	ΔH (kJ/kg)	Onset (°C)	ΔH (kJ/kg)
$NaNO_3$	305.7 (±0.09 %)	169.0 (±0.86 %)	304.9 (±0.05 %)	169.3 (±0.31 %)
Na_2SO_4-NaOH	280.0 (±1.10 %)	171.3 (±1.32 %)	278.1 (±0.21 %)	187.8 (±0.46 %)
LiOH-KOH	311.21	473.1 (±1.94 %)	313.67 (±0.07 %)	466.6 (±2.34 %)

a single PCM undergoing phase change over the 300 °C–450 °C temperature range.

Identified salts melting at constant temperature within the interval 300 °C–450 °C are ordered by decreasing latent heat in Table 6; these salts would be interesting for the cascade concept. Only those with relative volume expansion <19 % and latent heat higher than 100 kJ/kg were considered for later testing.

Table 6
Potential candidates to be used as storage media in the superheated steam module-Option A.

Formulae	Composition (wt%)	Melting point (°C)	Latent heat (kJ/kg)	Relative volume expansion (%)	Considered?
LiF-LiOH	21.33–78.67	431	889	3.8	Yes
LiOH-Li_2CO_3	63.55–36.45	424	786	1.7	Yes
LiOH-Li_2SO_4	42.52–57.48	295	591	3.7	Yes
LiCl-$MgCl_2$	49.65–50.35	447	401	35.6	No
LiOH-RbOH	37.72–62.28	363	393	None	Yes
LiF-LiBr	8.62–91.38	450	275	38.0	No
LiCl-KCl	45.25–54.75	352	267	31.0	No
KCl-$MgCl_2$	64.49–35.51	422	259	34.0	No
NaCl-$CoCl_2$	42.98–57.02	366	234	25.0	No
$MnCl_2$-NaCl	64.33–35.67	426	230	40.0	No
KOH-K_2SO_4	83.52–16.48	376.23	175	21.0	No
KOH	100	403.85	167	18.0	Yes
KCl-$MnCl_2$	54.68–45.32	417	166	15.0	Yes
K_2CO_3-KOH	22.13–77.87	365.59	165	20.0	No
LiCl-LiI	15.05–84.95	368	160	17.0	Yes
NaOH	100	320	159	19.0	Yes
LiF-LiI	3.73–96.27	414	138	13.0	Yes
$MgCl_2$-RbCl	21.65–78.35	446	135.7	28.0	No
KCl-$CoCl_2$	42.94–57.06	348	126	27.0	No
LiI-NaI	65.25–34.75	342	113	19.0	No
LiCl-$PbCl_2$	9.88–90.12	388	105	68.0	No
NaCl-$PbCl_2$	7.95–92.05	410	91	75.0	No
KCl-$PbCl_2$	7.05–92.95	420	78	77.0	No
	19.69–80.31	408	79	42.0	No
RbOH	100	383	76.5	None	No

Identified salts melting over the temperature range 300–450 °C, useful for the single PCM with spread melting concept, are ordered by decreasing latent heat in Table 7. As previously, those salts with relative volume expansion <18 % are considered for further testing. One notices very high enthalpy change values associated to the solid-liquid transformation of LiOH/LiBr, LiOH/KOH and LiOH/LiI, as well as relative volume expansion values <3 %.

4.3. Materials testing

According to the screening above, two binary systems appear as really interesting candidates for both the saturated steam and the superheated steam storage modules: LiOH-LiBr and LiOH-KOH. Notice that the interest of LiOH-LiI is limited to the superheated steam module (Table 8).

The data presented in Table 8 shows the best compromise regarding relative volume expansion and energy density. It is also less expensive than LiOH/LiBr. DSC tests were performed on LiOH/KOH at the composition required for the saturated steam module (46.05–53.95 wt %) and results achieved were discussed above. The DSC tests carried out on LiOH/KOH at the new composition required for the superheated steam module (78.92–21.08 wt%) are presented below.

Before that, let us examine the enthalpy variation of LiOH/KOH temperature as predicted by FactSage. One can observe in Fig. 9 a first

Table 7
Potential candidates to be used as storage media in the superheated steam module-Option B.

Formulae	Composition (wt%)	Melting point (°C)	Latent heat (kJ/kg)	Relative volume expansion (%)	Considered?
LiOH-LiBr	72.67–27.33	304–450	1250	3.0	Yes
LiOH-KOH	80.12–19.88	314–450	1110	0.5	Yes
LiI-LiOH	32.23–67.77	335–450	831	0.3	Yes
LiOH-LiCl	23.56–76.44	315–450	605	25.0	No
Na_2CO_3-NaOH	42.33–57.67	286–450	600	22.0	No
NaF-NaOH	8.55–91.45	310–450	490	20.0	No
NaOH-Na_2SO_4	42.55–57.45	294.4–450	482	24.5	No
NaCl-$NaNO_3$	15.44–85.56	298–450	469	21.0	No
NaF-$NaNO_3$	4.96–95-04	304–450	466	20.0	No
$NaNO_3$-Na_2SO_4	80.12–19.88	298.95–450	440	21.0	No
NaBr-$NaNO_3$	29.42–70.58	291–450	433	23.0	No
Na_2CO_3-$NaNO_3$	9.55–90.45	306–450	420	25.0	No
$FeCl_2$-$FeCl_3$	23.78–76.22	293.51–450	368	42.0	No
NaI-$NaNO_3$	53.85–46.15	286.64	321	26.5	No
LiCl-RbCl	48.22–51.78	312	312	30.0	No
KF-KNO_3	5.21–94.79	308–450	306	14.0	Yes
LiCl-CsCl	38.33–61.67	327	287	40.0	No
KCl-KNO_3	21.66–78.34	307–450	280	16.0	Yes
KBr-KOH	65.45–34.55	300	272	24.0	No
KNO_2-K_2CO_3	87.24–12.76	325–450	260	14.5	No
KNO_3-K_2SO_4	91.81–8.19	333–450	253	15.0	No
KBr-LiBr	28.74–71.26	327.9–450	247	34.0	No
	60.44–39.56	327.9–450	232	32.0	No
KBr-KNO_3	21.63–78.37	329–450	242	15.0	Yes
CsBr-LiBr	34.21–65.79	287–450	226	38.3	No
	80.33–19.67	309–450	132	40.5	No
RbCl-RbOH	42.95–57.05	311–450	200	20.0	No
LiI-KI	93.31–6.69	284.78–450	179	13.0	Yes
	38.46–61.54	284.78–450	168	22.0	No
CsF-$CsNO_3$	45.92–54.08	309–450	169	115.0	No

Table 8
Data for selected storage media materials.

Module	Formulae	Composition (wt%)	Melting point (°C)	Latent heat (kJ/kg)	Relative volume expansion (%)
Saturated steam	LiOH-LiBr	45.27–54.73	303.89	802.80	11.5
	LiOH-KOH	46.05–53.95	314	534.86	6.88
	LiOH-LiI	41.71–58.29	334	307.86	2.99
Superheated steam	LiOH-LiBr	72.67–27.33	304–450	1250	3.0
	LiOH-KOH	78.92–21.08	314–450	1095	2.0
	LiI-LiOH	32.23–67.77	335–450	831	0.3

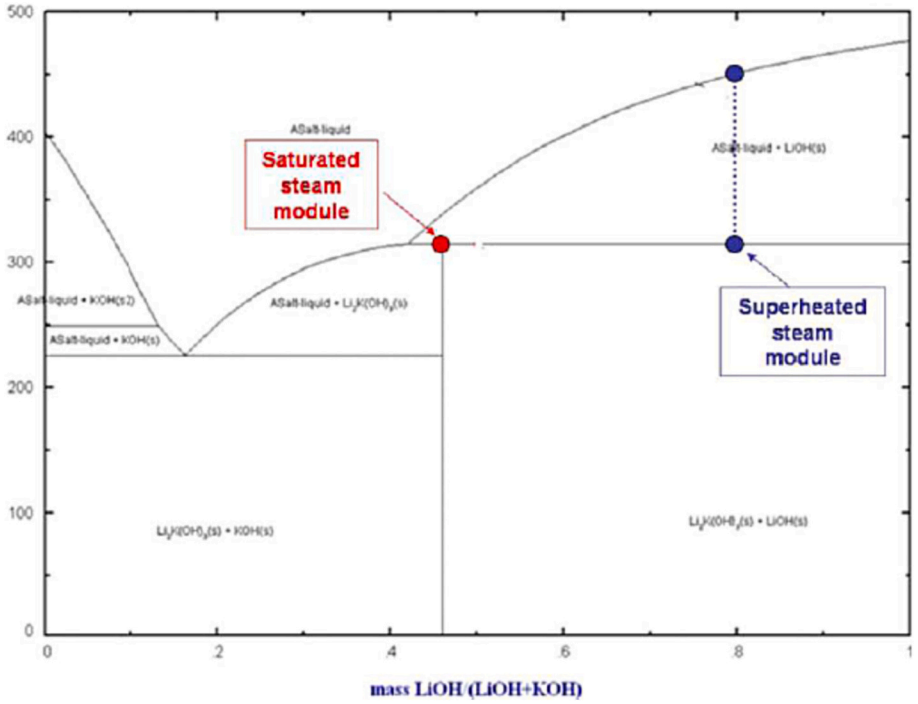

Fig. 9. Enthalpy-temperature function for 78.92 wt% LiOH-21.08 wt% KOH, obtained with FactSage.

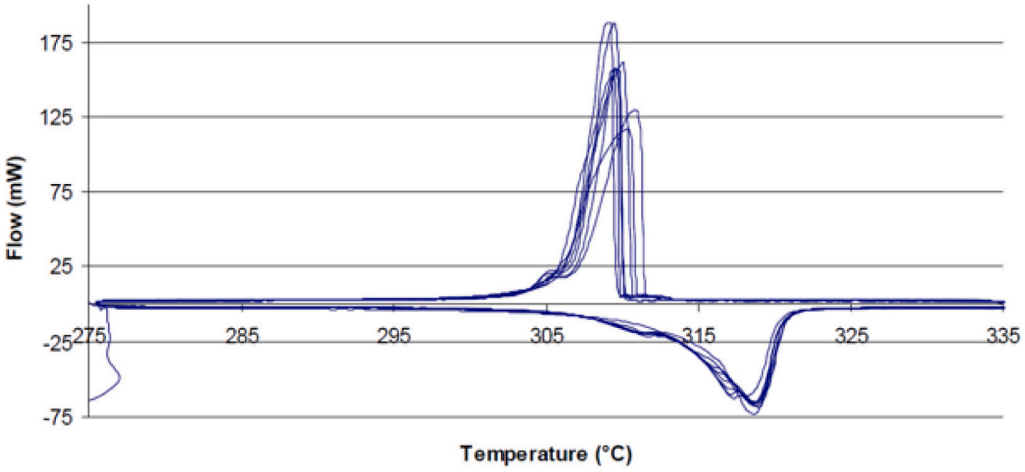

(a)

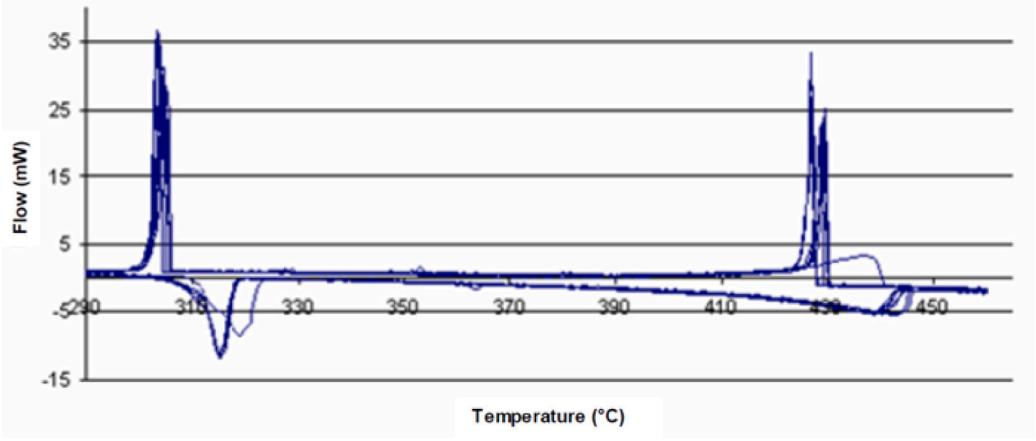

(b)

Fig. 10. Thermo-gram from DSC test carried out on a sample of binary LiOH-KOH. Heating/cooling rates: 1 °C/min heating/cooling rates. 10 melting/crystallization cycles. (a) 46.05 wt% LiOH, and (b) 78.92 wt% LiOH.

melting at 314 °C followed by a progressive melting from 314 °C to 450 °C. Enthalpy variation associated to the first melting is 209 kJ/kg ($\Delta V/V = 2.4$ %), while for progressive melting (sensible and latent heat) enthalpy variation is 885 kJ/kg ($\Delta V/V = -1.8$ %; negative value).

DSC were carried out on LiOH/KOH at the compositions selected for both storage modules, named, LiOH/KOH (46.05 wt% LiOH) for the saturated steam module and LiOH/KOH (78.92 wt% LiOH) for the superheated steam module. Thermo-grams achieved are presented in Fig. 10, respectively. In both cases one observes a good repetitiveness and reduced undercooling. Indeed, the form of the thermo-grams is as expected for melting at constant temperature (Fig. 10a, one-single pick) and for progressive melting (Fig. 10b). One notices too that there is no chemical components segregation during crystallization of LiOH/KOH (78.92 wt% LiOH). In fact, density of LiOH (solid) is close enough to the density of the liquid salt for gravity does not provoke segregation. This material had already been considered in other studies [19], allowing us to validate the methodology followed.

Although corrosion aspects are outside the scope of this study, their analysis is important and should be considered. This is justified by the enormous number of existing studies referring to the use of hydroxides as PCM in high temperature applications [20–22].

5. Conclusions

A direct steam generation (DSG) CSP plant holds the potential to achieve markedly higher overall thermal efficiency in comparison to existing molten salt or thermal oil CSP plants. This is owing to DSG direct production of steam for electricity generation, obviating the necessity for intermediate heat exchangers or fluid systems, thereby minimizing energy losses. Furthermore, DSG streamlines plant design and diminishes maintenance demands by eliminating the need for heat transfer fluids like molten salt or thermal oil. The technology advantages can be further amplified through the development of extended-duration thermal storage systems, enabling discharge while maintaining nominal cycle conditions. The utilization of a phase change material in conjunction with a two-tank molten salt solution emerges as a feasible design approach, particularly in the context of employing LiOH/KOH. Despite the notable challenge of corrosion, this choice presents a range of advantages:

- Remarkably high enthalpy variations inherent in full solid-liquid transformations yield notably compact storage systems, it has 5–10 times more energy density compared to traditional solutions.

- Minimal volume expansion, 2–7 %, during the melting process serves to significantly mitigate mechanical concerns as previously observed in graphite/salt composites, bolstering system reliability.
- The technology demonstrates exceptionally low subcooling tendencies, further enhancing its efficiency and effectiveness.
- In the case of LiOH/KOH (78.92–21.08 wt%), the absence of segregation during Differential Scanning Calorimetry (DSC) tests underscores its viability. Moreover, FactSage predictions closely align solid and liquid phase density values, reaffirming the model's accuracy.
- Notably, the system reliance on merely two chemical components, LiOH and KOH, underscores its simplicity and efficiency. This streamlined composition holds significant potential for facilitating industrial scalability and commercial viability.

The specified temperatures outlined in this study aim to mirror the behaviour of indirect storage in DSG. These values should be verified through a more comprehensive performance model, which necessitates a detailed assessment of cycle efficiency. The temperature profile will be contingent on the module designs and the pitches acquired in the heat exchangers. The subsequent phase of our work will focus on designing these equipment components, considering factors such as heat transfer coefficients and other essential properties, including thermal diffusivity.

CRediT authorship contribution statement

Cristina Prieto: Writing – review & editing, Writing – original draft, Supervision, Resources, Project administration, Methodology, Investigation, Funding acquisition, Formal analysis, Data curation, Conceptualization. **Luisa F. Cabeza:** Writing – review & editing, Writing – original draft, Formal analysis, Conceptualization. **M. Carmen Pavón-Moreno:** Writing – review & editing, Visualization. **Elena Palomo:** Validation, Supervision, Methodology, Investigation, Formal analysis, Data curation.

Declaration of competing interest

The authors declare that they have no known competing financial interests or personal relationships that could have appeared to influence the work reported in this paper.

Data availability

The data that has been used is confidential.

Acknowledgements

This work was partially funded by the Ministerio de Ciencia e Innovación de España [(TED2021-132216A-I00) (ITC-20111061-FEDER-Innterconecta-Composol), (PID2021-123511OB-C31 - MCIU/AEI/FEDER, UE), and (RED2022-134219-T)].

The authors at University of Lleida would like to thank the Catalan Government for the quality accreditation given to their research group GREiA (2017 SGR 1537). GREiA is a certified agent TECNIO in the category of technology developers from the Government of Catalonia. This work is partially supported by ICREA under the ICREA Academia programme.

References

[1] U.S.D. of Energy, Energy Storage Grand Challenge Roadmap, 2020.
[2] E. González-Roubaud, D. Pérez-Osorio, C. Prieto, Review of commercial thermal energy storage in concentrated solar power plants: steam vs. molten salts, Renew. Sust. Energ. Rev. 80 (2017) 133–148, https://doi.org/10.1016/j.rser.2017.05.084.
[3] T. Hirsch, A. Khenissi, A systematic comparison on power block efficiencies for CSP plants with direct steam generation, in: Energy Procedia, Elsevier Ltd, 2014, pp. 1165–1176, https://doi.org/10.1016/j.egypro.2014.03.126.
[4] M. Alguacil, C. Prieto, A. Rodriguez, J. Lohr, Direct steam generation in parabolic trough collectors, Energy Procedia 49 (2014) 21–29, https://doi.org/10.1016/j.egypro.2014.03.003.
[5] M. Ploquin, S. Mer, A. Toutant, F. Roget, CFD investigation of level fluctuations in steam accumulators as thermal storage: a direct steam generation application, Sol. Energy 245 (2022) 11–18, https://doi.org/10.1016/j.solener.2022.08.048.
[6] A.A. Al Kindi, A.M. Pantaleo, W. Kai, C.N. Markides, Thermodynamic assessment of steam-accumulation thermal energy storage in concentrating solar power plants, in: International Conference on Applied Energy 2019, Västerås, Sweden, 2019 (pp. Paper ID: 1077).
[7] A. Ehtiwesh, C. Kutlu, Y. Su, S. Riffat, Modelling and performance evaluation of a direct steam generation solar power system coupled with steam accumulator to meet electricity demands for a hospital under typical climate conditions in Libya, Renew. Energy 206 (2023) 795–807, https://doi.org/10.1016/j.renene.2023.02.075.
[8] A.H. Alami, A.G. Olabi, A. Mdallal, A. Rezk, A. Radwan, S.M.A. Rahman, S.K. Shah, M.A. Abdelkareem, Concentrating solar power (CSP) technologies: status and analysis, Int. J. Thermofluids 18 (2023) 100340, https://doi.org/10.1016/j.ijft.2023.100340.
[9] NREL, Concentrating Solar Power Projects With Operational Plants, 2020.
[10] R. Osuna, V. Fernandez, M. Romero, M.J. Blanco, PS10: A 10 MW Solar Tower Power Plant for Southern Spain. Final Technical Progress Report for NNE5-1999-356 Contract With the European Commission, 2006.
[11] C. Prieto, A. Rodríguez, D. Patiño, L.F. Cabeza, Thermal energy storage evaluation in direct steam generation solar plants, Sol. Energy 159 (2018) 501–509, https://doi.org/10.1016/j.solener.2017.11.006.
[12] T.B.J.B.D.L.H.M.-S.W.-D.S. Rainer Tamme, Latent Heat Storage Above 120°C for Applications in the Industrial Process Heat Sector and Solar Power Generation, 2007.
[13] G.J. Janz, Molten Salts Handbook, Academic Press, 1967.
[14] J.F. Shackelford, W. Alexander, The CRC Materials Science and Engineering Handbook, CRC, 1991.
[15] J. Lopez, Nouveaux Matériaux Graphite/Sels pour le Stockage d'Energie Thermique à Haute Température. Etude des Propriétés de Changement de Phase, Université Bordeaux, 2007, p. 1.
[16] C. Zhang, Y. Han, Y. Wu, Y. Lu, Comparative study on high temperature thermal stability of quaternary nitrate-nitrite mixed salt and solar salt, Sol. Energy Mater. Sol. Cells 230 (2021), https://doi.org/10.1016/j.solmat.2021.111197.
[17] A.F. Elmozughi, L. Solomon, A. Oztekin, S. Neti, Encapsulated phase change material for high temperature thermal energy storage - heat transfer analysis, Int. J. Heat Mass Transf. 78 (2014) 1135–1144, https://doi.org/10.1016/j.ijheatmasstransfer.2014.07.087.
[18] C. Martin, T. Bauer, H. Müller-Steinhagen, An experimental study of a non-eutectic mixture of KNO3 and NaNO3 with a melting range for thermal energy storage, Appl. Therm. Eng. 56 (2013) 159–166, https://doi.org/10.1016/j.applthermaleng.2013.03.008.
[19] F.J. Ruiz-Cabañas, A. Jové, C. Prieto, V. Madina, A.I. Fernández, L.F. Cabeza, Materials selection of steam-phase change material (PCM) heat exchanger for thermal energy storage systems in direct steam generation facilities, Sol. Energy Mater. Sol. Cells 159 (2017) 526–535, https://doi.org/10.1016/j.solmat.2016.10.010.
[20] M. Walczak, F. Pineda, Á.G. Fernández, C. Mata-Torres, R.A. Escobar, Materials corrosion for thermal energy storage systems in concentrated solar power plants, Renew. Sust. Energ. Rev. 86 (2018) 22–44, https://doi.org/10.1016/j.rser.2018.01.010.
[21] M.M. Kenisarin, High-temperature phase change materials for thermal energy storage, Renew. Sust. Energ. Rev. 14 (2010) 955–970, https://doi.org/10.1016/j.rser.2009.11.011.
[22] S. Bell, T. Steinberg, G. Will, Corrosion mechanisms in molten salt thermal energy storage for concentrating solar power, Renew. Sust. Energ. Rev. 114 (2019), https://doi.org/10.1016/j.rser.2019.109328.